Experimental Study of Isothermal Swirling Flows in a Dump Combustor

M. Samimy* and C. A. Langenfeld†
Ohio State University, Columbus, Ohio

Detailed mean and turbulence data were obtained in a dump combustor with and without swirling inlet flow. A two-component LDV was used, and large samples were collected to resolve the second- and third-order correlations of velocity fluctuations with good accuracy. Large-amplitude well-organized oscillations were observed in the swirling flows and discussed. The swirling flows with and without vortex breakdown exhibited significantly different mean flow and turbulence field behavior.

Nomenclature

H = step height
k = turbulence kinetic energy
R = radial coordinate
S = swirl number, Eq. (1)
SIG = standard deviation
U,W = mean axial and azimuthal velocities
u,w = axial and azimuthal rms velocity fluctuations
U_{ref} = inlet pipe centerline velocity
X = axial coordinate

Subscripts

h = hub of the swirler
i = inlet pipe
u = axial component
w = azimuthal component

I. Introduction

SWIRLING flows have been the subject of extensive research efforts in a wide variety of engineering disciplines. Continuous combustion devices such as furnaces, gas turbines, and ramjet engines are but a few examples. Concentrated efforts have been expended for understanding and characterizing combustion processes of various geometries and concepts. Combustor engineers have designed and implemented swirl devices in many of their combustors in order to assist fuel-air mixing, to enhance flame stabilization, to improve blowoff limits, and to increase combustion efficiency.[1-14]

Different concepts such as free jets,[4,5] coaxial confined jets,[3,6-9] multijet tangential entries,[10] and a single confined jet expanding into a larger tube[1,2,11,12] have been used to investigate swirling flows. Methods of swirl generation and characterization have been discussed in detail by Beer and Chigier[13] and by Gupta et al.[14] Buckley et al.[1] have shown the considerable impact of different swirl profiles (i.e., forced vortex, free vortex, and constant angle) on the efficiency and pressure recovery of dump combustors. Kilik[15] has shown significant effects of swirl vane angle curvature on the induced recirculation size. The majority of the research to date has the common goal of increasing the understanding of such complex flowfields and improving the accuracy of the computational techniques to reduce the expensive cut-and-try approach to combustor design. However, progress has been slow due to the complex three-dimensional nature of this type of flowfield. The current predictive codes make various closure assumptions in the solution of Navier-Stokes equations. Computational modelers still require detailed experimental data for improving and refining their closure models.

There is an obvious lack of detailed experimental data due to the insufficiencies of experimental techniques and/or improper documentation of the results. Optical diagnostic techniques experience optical aberration introduced by the curved combustor wall.[16] Lack of proper optical access for making measurements in complex geometries is also a great problem. Accuracy of conventional intrusive instruments such as hot wires and pitot probes are questionable in swirling flows.[6] These measurements suffer from directional ambiguity and flow disturbance. Also, the inability of these instruments to cope with high levels of turbulence fluctuations is of great concern.

The purpose of this study was two-fold: first, to explore isothermal swirling flows and to aid in understanding the physical processes, and second, to establish a benchmark set of experimental data for turbulence model development and assessment.

II. Experimental Facility

Dump Combustor Model

All experiments were conducted in a clear plastic cold-flow model of a ramjet dump combustor schematically shown in Fig. 1. The combustor model consisted of two major segments: the inlet assembly and the combustor chamber and contraction nozzle section. The inlet assembly consisted of the following sections: a 300-mm-diam settling chamber; an inlet pipe, 2.85 m in length and 101.6 mm i.d.; a cylindrical teflon swirl housing, 104.5 mm i.d., 152.4 mm o.d., 154 mm in length. The combustion chamber and contraction nozzle section consisted of a tube 1.85 m in length and 152.4 mm i.d. connected to a 30 deg converging nozzle with a 44% exit area. The unique feature of the research combustor was that the inlet assembly was supported on an elaborate traversing system controlled by a stepping motor. The entire inlet tube and the teflon swirl housing were capable of sliding through and traversing the length of the combustor chamber with a resolution of 0.025 mm. Two flat optical windows, 38 × 38 mm, were used for coincident two-component LDV measurements. One window was located on the inlet tube 94 mm upstream of the swirler. In order to introduce undisturbed flow to the swirler, a

Received June 12, 1987; revision received Nov. 24, 1987.

*Assistant Professor, Department of Mechanical Engineering. Member AIAA.
†Graduate Student, Department of Mechanical Engineering.

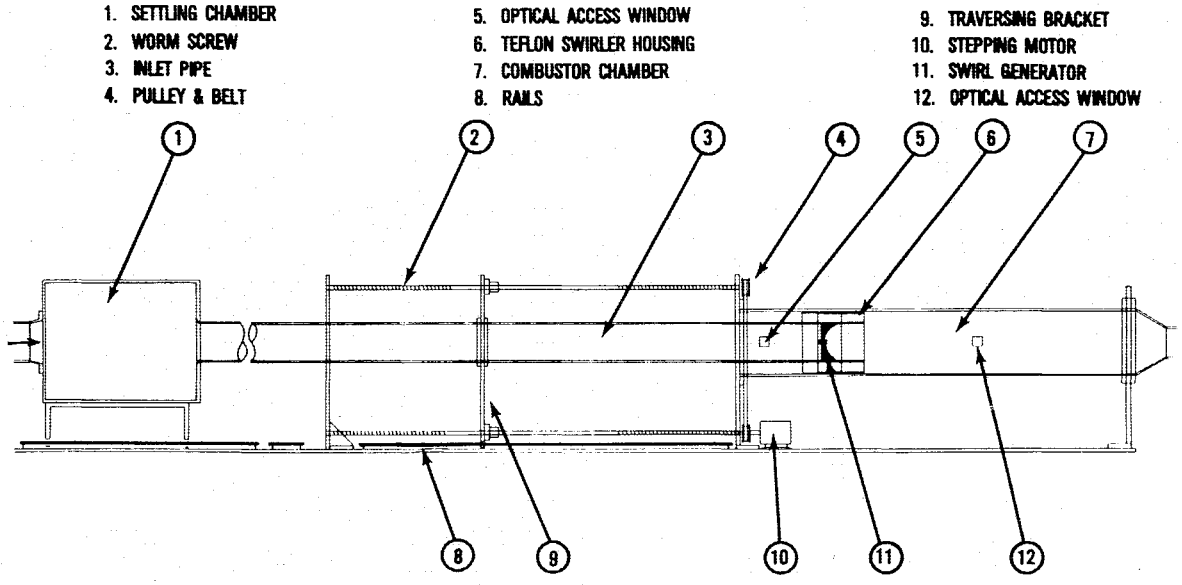

Fig. 1 Schematic of the experimental facility.

contoured plug was fabricated that replaced the optical flat window when upstream flow measurements were not being performed. The second window was located on the combustor wall at 5.7 combustor diameters upstream of the contraction nozzle. There was a maximum of 0.8 mm discontinuity between this flat window and the combustor wall, which generated some disturbances. Experiments showed that these disturbances were limited to regions very close to the combustor wall. Based on Lilley's results,[2] the effect of contraction nozzle on the flowfield at the measurement stations was believed to be insignificant. A series of experiments were conducted without the contraction nozzle in place. The measurements obtained with and without the contraction nozzle in place were identical, which confirmed Lilley's results. With this arrangement, optical aberration was avoided, and at the same time flow disturbances were kept to an absolute minimum.

Two constant-angle axial flow-type swirl generators with swirl numbers of 0.3 and 0.5 were used. The swirl number is defined as

$$S = \int_{R_h}^{R_i} UWr^2\,\mathrm{d}r \Big/ \left(R_i \int_{R_h}^{R_i} U^2 r\,\mathrm{d}r \right) \qquad (1)$$

where R_h and R_i are the hub and outer-ring radii. Each swirler had 12 curved inlet guide vanes, welded between a 101.6 mm i.d. outer ring and 19 mm o.d. central hub. In this study, the swirlers were located 50 mm upstream of the dump plane.

Air was pushed through the model by a centrifugal-type blower. Throughout these experiments, the inlet centerline velocity was monitored continuously with a pitot probe located 266 mm upstream of the inlet pipe access window and was kept at 19.2 ± 0.4 m/s corresponding to a Reynolds number of 125,000 based on the combustor inlet diameter.

Laser Doppler Velocimeter

A TSI, Inc., frequency-counter-based two-component coincident LDV system was used for velocity measurements. The optical system that was operated in the back-scatter mode used two frequency shifters and a $3.75X$ beam expander with 35 mm entrance beam spacing. The 514.5 nm and 488 nm lines of an argon ion laser operating at 300 mW were used for all measurements. The LDV probe volume diameter and length were approximately 80 μm and 600 μm, respectively. To provide directional sensitivity and to prevent fringe bias, both sets of fringes were shifted at 40 MHz corresponding to fringe velocities of approximately 73 m/s.

Titanium tetrachloride vapor was entrained by dry air and mixed with saturated air in a reaction chamber to generate solid titanium dioxide particles of less than one micron in diameter for seeding the flow.[17] To approach a uniformly seeded flow, titanium dioxide particles were introduced into a reservoir upstream of the blower. Typical data rate in each channel was between 5000–10,000/s, which gave a coincident data rate of 2000–6000/s with a 20 μm coincidence window. In order to reduce statistical uncertainties, especially for the higher-order moments of turbulence fluctuations, a minimum of 27,300 samples/channel were collected at each measurement location in the flowfield.

Dual-Channel FFT Analyzer

A model 660A Nicolet Scientific Corporation dual-channel FFT analyzer was used to obtain power spectral densities of both the turbulence and acoustic fields. A sample/hold fashion analog signal that was equal to approximately $0.7(U + W)$ was obtained from the LDV counter processor for spectral analysis. Also, a 4-mm-diam microphone located outside of the combustor chamber wall was used for obtaining analog acoustic signal.

III. Experimental Results and Discussions

Velocity Bias Correction

Although LDV has been routinely used, the associated statistical bias problems are dealt with on the basis of individual experimental conditions. In isothermal low-speed flows such as the one under consideration, velocity bias is the only major concern. Originally, McLaughlin and Tiederman showed that individual realization LDV sampling is biased toward higher velocities and offered a procedure for its correction.[18] Since then many other techniques have been developed for velocity bias correction.[17,19-21]

Three bias-correction schemes were investigated in these experiments. The three techniques were: particle interarrival time weighting, constant-time interval sampling, and the extended inverse two-dimensional velocity weighting of McLaughlin and Tiederman. The particle interarrival time weighting was expected to work properly, since the coincident sample rate was between 2000–6000/s and higher than the expected time scale of large-scale structures in the flowfield.[22] The constant-time interval sampling has been proven to be an effective tool for velocity bias correction as long as the sampling rate is an order

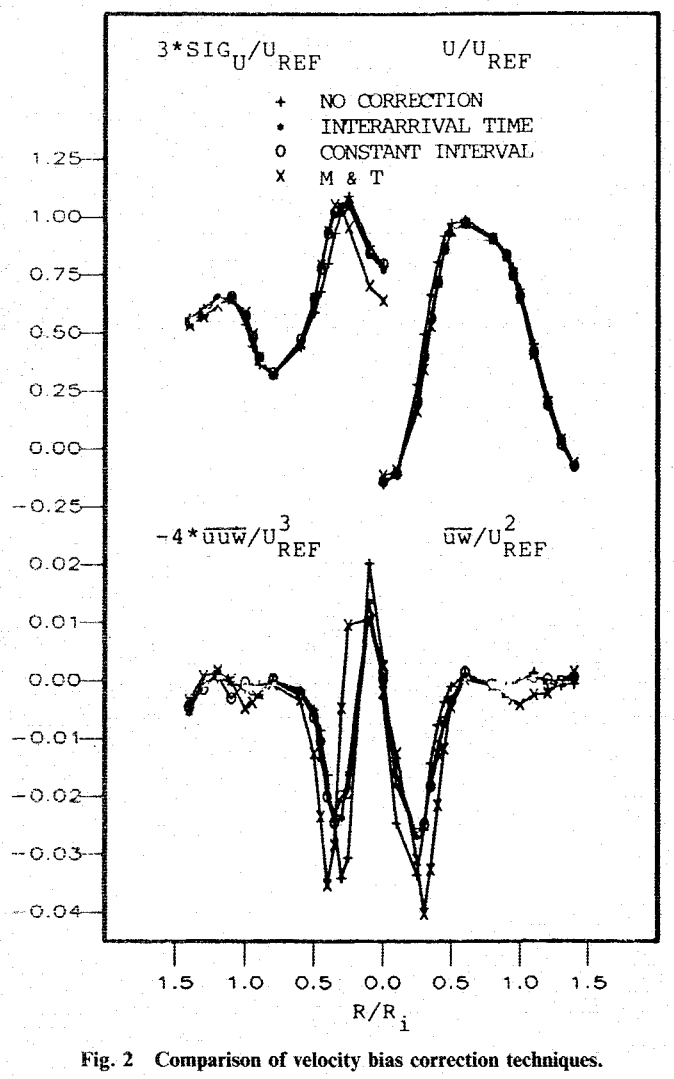

Fig. 2 Comparison of velocity bias correction techniques.

of magnitude less than the valid data rate.[17,21] In the present experiments, this criterion was satisfied; therefore, this technique was anticipated to perform properly.

In flowfields with possible simultaneous zero or near-zero velocities in both channels, McLaughlin and Tiederman correction overcompensates the velocity bias by providing very large weighting coefficients.[19] Since there are many regions in the present flow with small values of both velocity components, this technique was not expected to be appropriate.

Figure 2 shows the experimental results for the mean axial velocity and rms velocity fluctuations, Reynolds stress, and one component of third-order mean products of velocity fluctuations at 2 step heights downstream of the dump plane for $S = 0.5$. For this specific case, the measurements were carried out only in one side of the centerline; however, the results are plotted in both sides only for clarity.

There is an excellent agreement between mean velocities and turbulence data of the constant-time interval sampling and the particle interarrival time weighting methods. As expected, the uncorrected mean velocities show higher values everywhere in the flow with no distinct trend in turbulence intensities.

At this location in the flow, there is a large central recirculation zone with small mean axial and tangential velocities, hence a high probability of an infinite weighting factor in the McLaughlin and Tiederman method. Initially, no upper limit was set for this weighting factor, which produced near-zero mean velocities and turbulence intensities from the centerline up to 0.5 step height from the centerline. Then, the maximum weighting factor was set arbitrarily at 10^4, which produced the results shown in Fig. 2. This correction scheme and the associated problems are discussed in detail by Petrie et al.[19]

There is an excellent agreement between shear stress and triple products of velocity fluctuations results of the constant-time interval sampling and those of the particle interarrival time weighting. Nejad and Davis[21] have shown similar agreement between the shear stress results of these two schemes, and also analytical results obtained in the self-similar region of a free jet. All of these are indications that both correction schemes work properly. Unfortunately, both of these techniques require very high data rate, which is difficult to obtain in cases such as combustion[3] and supersonic flows.[23,24] The two other techniques, the uncorrected and the McLaughlin and Tiederman's, provide absolute values of shear stress and triple products of velocity fluctuations up to 50% higher or lower than those of constant-time interval sampling technique, depending on the measurement location.

In conclusion, particle interarrival time correction was selected over the other techniques. This technique was chosen over the constant-time sampling, because its sample size was roughly 10 times larger, 27,300 per channel as compared to 2700 per channel, therefore, resulting in a lower statistical uncertainty.

To further verify the validity of the measurements, axial velocity profiles at each station were integrated to determine the mass flux through the model. The agreement between upstream and downstream mass flow rates were better than 4%.

Incoming Flow

In order to isolate and identify the effects of swirl on the combustor flowfield, upstream flow conditions must be well understood and documented. As discussed earlier, a 38 × 38 mm optical access flat window located 94 mm upstream of the swirler housing was used for incoming flow measurements. The length of the inlet pipe from the settling chamber to the measurement location was approximately 2.8 m.

Figure 3 shows the mean axial velocity and the axial and tangential rms velocity fluctuations, normalized with respect to the inlet centerline velocity. The inlet centerline velocity was obtained using a pitot probe located approximately 20 cm upstream of the LDV measurement location.

Rms velocity fluctuations profiles are typical of a fully developed pipe flow; lower intensities at the center, approximately 4% tangential and 5% axial intensities, increasing toward the side walls, 7% tangential and 9% axial intensities. The axial rms velocities are higher than the tangential rms velocities, but the anisotropic ratio is almost constant, between 1.3 and 1.4, throughout the inlet pipe.

Mean Flow Result

Within the dump combustor, a total of 13 axial locations were used to collect mean and turbulence data for each of the three swirl conditions analyzed in this paper. The first location was 0.38 step height from the dump plane. This was the closest location at which the two-component LDV could be used without the teflon swirler housing intercepting the laser beams. At this location, only one-half of the profile could be obtained. In all other locations, profiles were obtained on both sides of the combustor centerline. Figure 4 shows the axial mean velocity profiles in selected streamwise locations for the three swirl levels.

The profiles in Fig. 4, for the flow without swirl, are typical of both axisymmetric[2] and two-dimensional[25] backstep flows: very slow decay of the core flow and recirculation in the base region. Reattachment occurred approximately 8 step heights downstream of the dump plane, which is in close agreement with similar axisymmetric[2] and two-dimensional[26] configurations with fully turbulent inlet flows.

Comparison of the results in Fig. 4 shows the significant impact of swirl on the mean flowfield. The length of corner recirculation zone has decreased from approximately 8 step

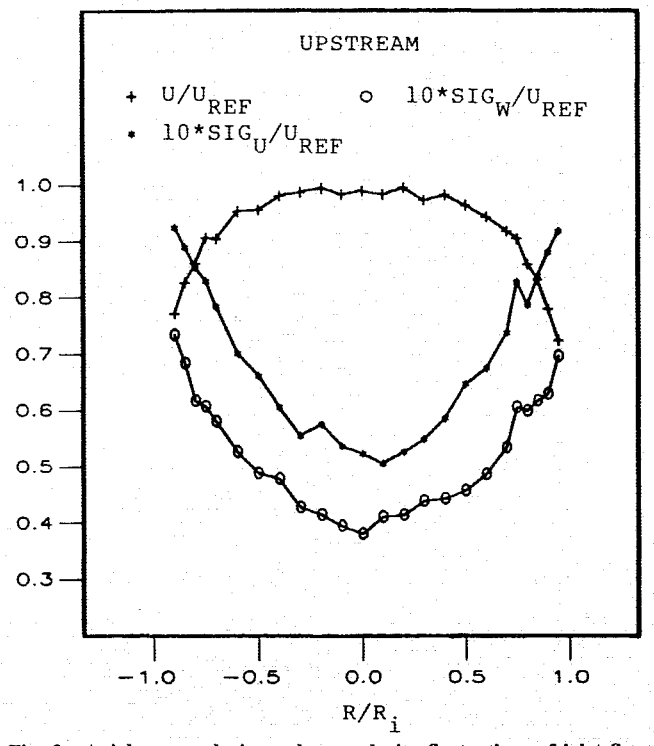

Fig. 3 Axial mean velocity and rms velocity fluctuations of inlet flow prior to swirl generator.

heights for the flow with no swirl to about 4.3 step heights for $S = 0.3$ and to about 3.2 step heights for $S = 0.5$ swirling flow. This decrease in corner recirculation length, which is caused by rapid expansion of flow after separation due to centrifugal forces, has also been reported by Lilley.[2]

In vortex flows, depending upon the Reynolds number and also the strength of the vortex, a phenomenon may occur that is termed vortex breakdown. Vortex breakdown is followed by a flow reversal region and a region of chaotic flow.[2,3,27–29] In the present experiments, for $S = 0.3$ there is a large flow deceleration at the core of the vortex, but apparently it is not strong enough to cause vortex breakdown. For $S = 0.5$, vortex breakdown has occurred upstream of the dump plane and the central recirculating flow extended approximately 4.4 step heights downstream of the step. The maximum diameter of the central recirculating region is about 0.8 step heights and located about 3 step heights from the dump plane. Lilley[2] has shown the significant effects of swirl strength and also downstream contraction nozzle location and contraction ratio on the size and the shape of the recirculation region. Another important difference between the two swirling flows is the axial velocity gradient at the centerline, which is much higher for the stronger swirling flow than for the weaker swirling flow.

Figure 5 shows the tangential velocity profiles for both swirling flows. Although initially both flowfields show profiles typical of a dump combustor flow[2] and also similar to lifting surface leading-edge or trailing-edge vortex flows,[28,29] they show totally different behavior further downstream. The stronger swirling flow keeps the strength of its vortex core all the way to the last measurement location, 24 step heights downstream. This is consistent with the earlier results for similar or even stronger swirling flows.[2] The weaker swirling flow expands its vortex core at the expense of losing its strength; the flow becomes a forced vortex after about 10 to 12 step heights from the dump plane. This deformation of vortex and its probable cause will be discussed later. For $S = 0$, tangential velocity was almost zero everywhere in the flowfield.

Turbulence Results

Figure 6 shows the axial rms velocity fluctuations for three swirl levels. Flow with no swirl shows local peak values of rms

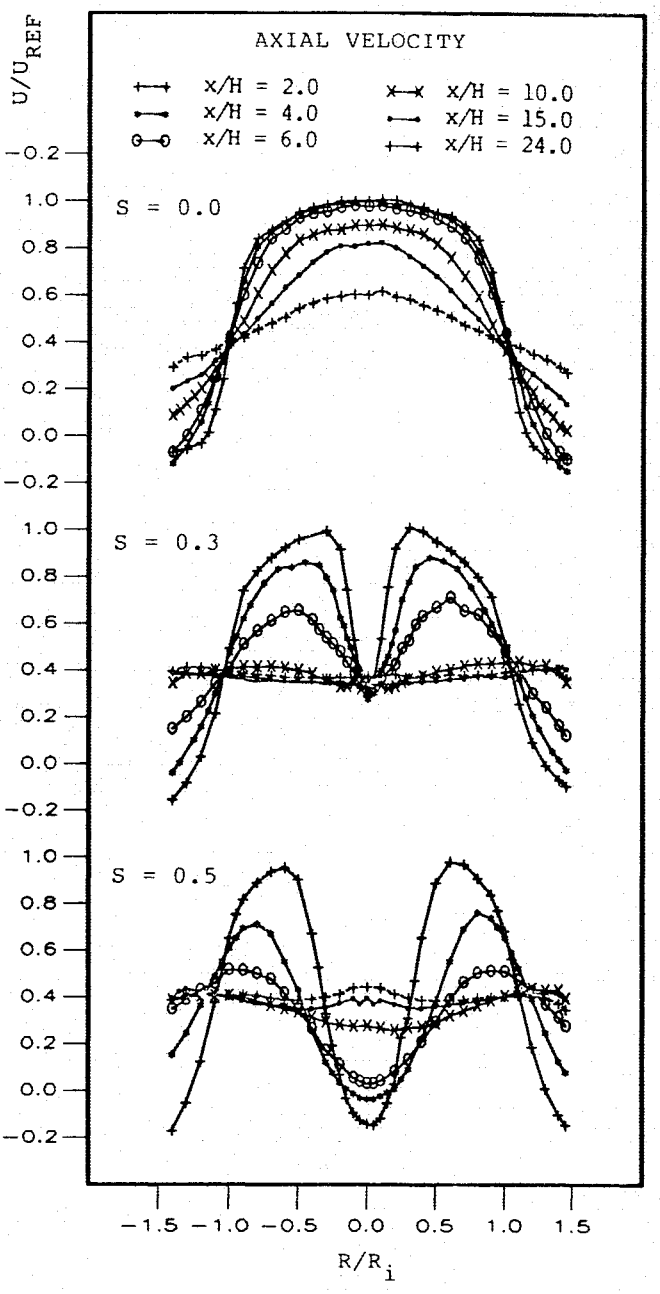

Fig. 4 Axial mean velocity profiles.

velocities in the shear layer generated between the core flow and the corner recirculating flow and also shows very slow decay in the streamwise direction. These results agree with those of Lilley[2] and show good similarity with the results of similar two-dimensional backstep flows.[25,26] The swirling flows show two local peaks, one in the shear layer at the edge of the vortex core, the other in the shear layer generated by the recirculating flow. The decay of rms velocity fluctuations is extremely rapid in the streamwise direction, especially for the stronger swirling flow, which is an indication of rapid diffusion and dissipation. The maximum axial rms velocity fluctuations in the corner recirculating flow generated shear layer for all three swirl levels occur before the reattachment and are followed by a rapid decay. This behavior is typical of two-dimensional flows with no swirl.[26,30,31] The general consensus is that the large-scale structures in the shear flow approaching the wall interact with the wall and breakdown.[26] Based on the present results, this seems to be the case in even swirling flows.

Contrary to expectation, the axial rms velocity fluctuations within the shear layer generated by the corner recirculating

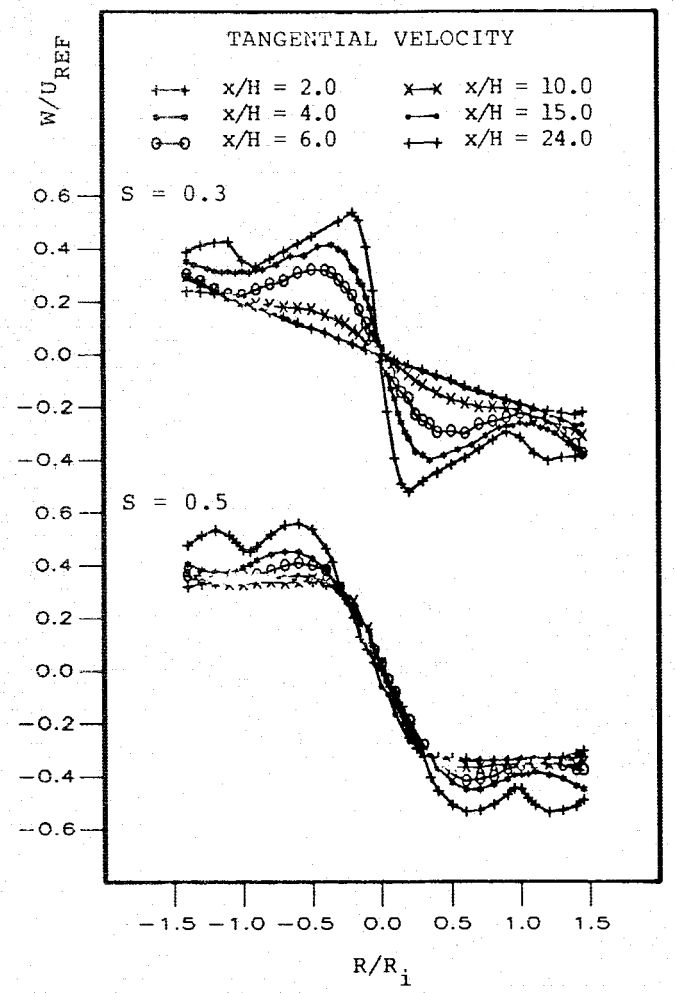

Fig. 5 Tangential mean velocity profiles.

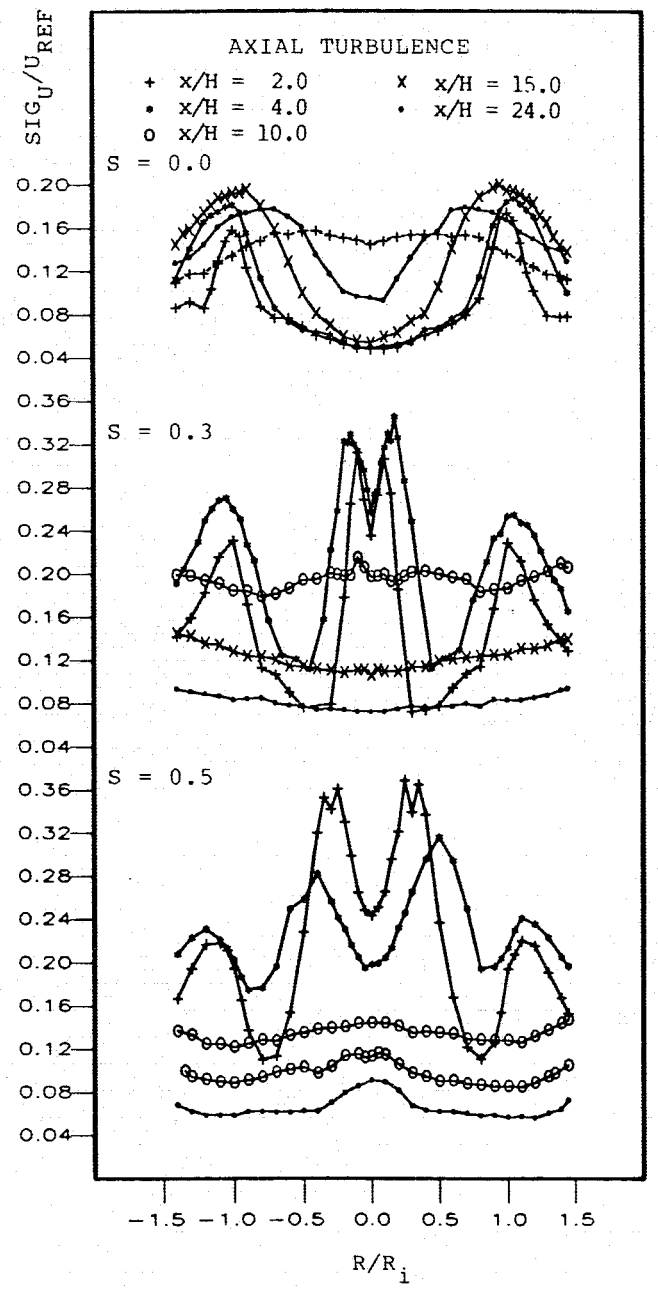

Fig. 6 Axial rms velocity fluctuations profiles.

flow for $S = 0.3$ is higher than that of $S = 0.5$. Both random and organized fluctuations contribute to the measured rms velocity functuations. As it will be shown later, there are highly coherent structures within both swirling flows that contribute to these high intensities, but the energy level of these coherent structures is almost an order of magnitude higher for $S = 0.3$, which could explain the higher rms fluctuations.

Figure 7 shows the tangential rms velocity fluctuations for three swirl levels. For flow with no swirl, the tangential rms fluctuations behave similarly to those of axial rms fluctuations. The anisotropic ratio varies between 1.1 and 1.5 and consistently peaks around one step height from the centerline. For both swirling flows, the peak rms fluctuations occur in the core of the vortex. As it was shown in the mean flow results, the vortex core for $S = 0.3$ expands and finally covers the entire combustor diameter; as a result, the peak rms fluctuations decay, and finally the tangential rms fluctuations become uniform across the combustor. For $S = 0.5$, the decay of the vortex core peak rms fluctuations occur only within the central recirculation zone. The anisotropic ratio varies significantly in the flowfield, and for the stronger swirling flow it does drop to as low as 0.5 in the vortex core further downstream in the flow.

Figure 8 shows Reynolds stress profiles for both swirling flows. In both flows, local peaks occur within the wall boundary layer, the shear layer generated by the recirculating flow, and at the edge of the vortex core. Very high Reynolds stresses at the edge of the vortex core are a reflection of strong shear forces between vortex core and the outer flow. This has also been shown by Lilley.[2] The higher Reynolds stress for weaker swirling flow at the edge of the vortex core could be due to two factors. The first factor is the stronger vortex core for the weaker swirling flow up to about 4 step heights downstream of the dump plane (see Fig. 5). The second factor is the well-organized large-scale oscillations in the weaker swirling flow, which will be discussed shortly. The Reynolds stress values for the no-swirl case are over 20 times less than those of swirling flows.

Figures 9 and 10 show triple products of velocity fluctuations for both swirling flows. Extremely large values of these correlations, especially for $S = 0.3$, confirm existence of organized structures in these flows. The $uuu + uww$ and $uuw + www$ terms could be interpreted as the convection of turbulent kinetic energy by large-scale structures in the axial and tangential directions, respectively. Positive and relatively small values of axial convection around the vortex core, and negative and relatively large values around the edge of the vortex core in both flows, are in accord with the slow development of the mean axial field at the center and the fast development at the edge of the vortex core.

The tangential convection term (Fig. 10) at the edge of the vortex core for $S = 0.3$ is very high initially but decays to negligible values after about 6 step heights. For $S = 0.5$, this term is lower initially but is persistent all the way up to 24 step

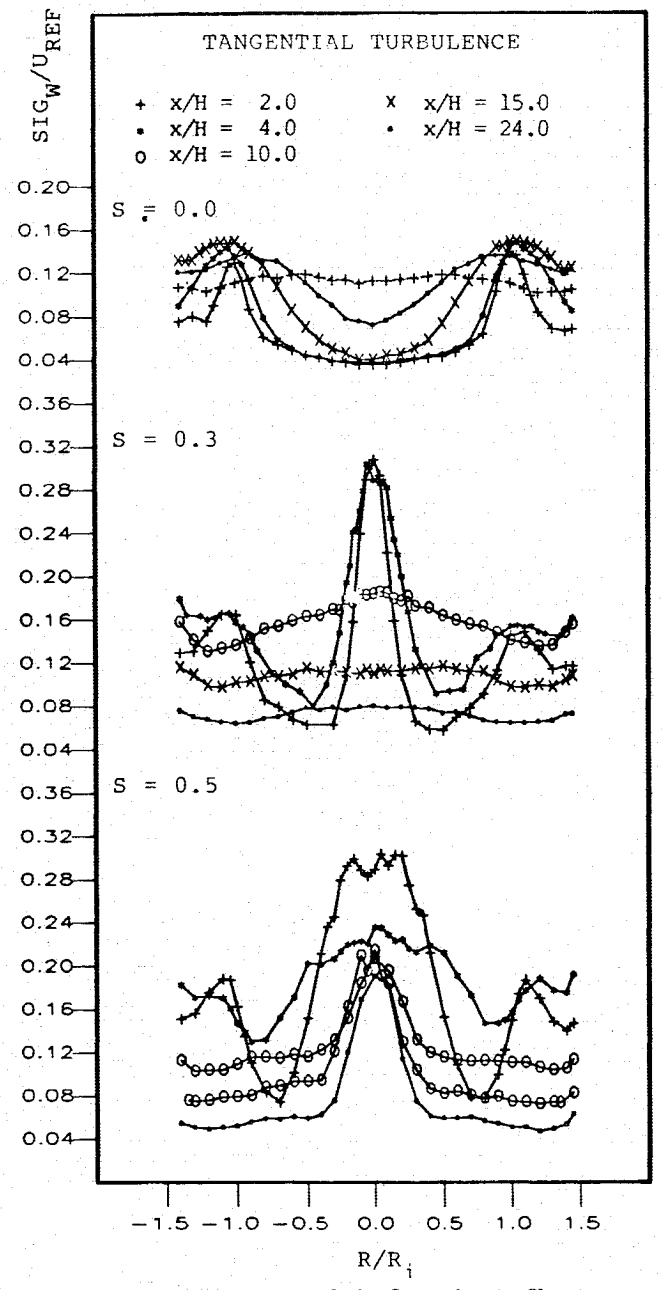

Fig. 7 Tangential rms velocity fluctuations profiles.

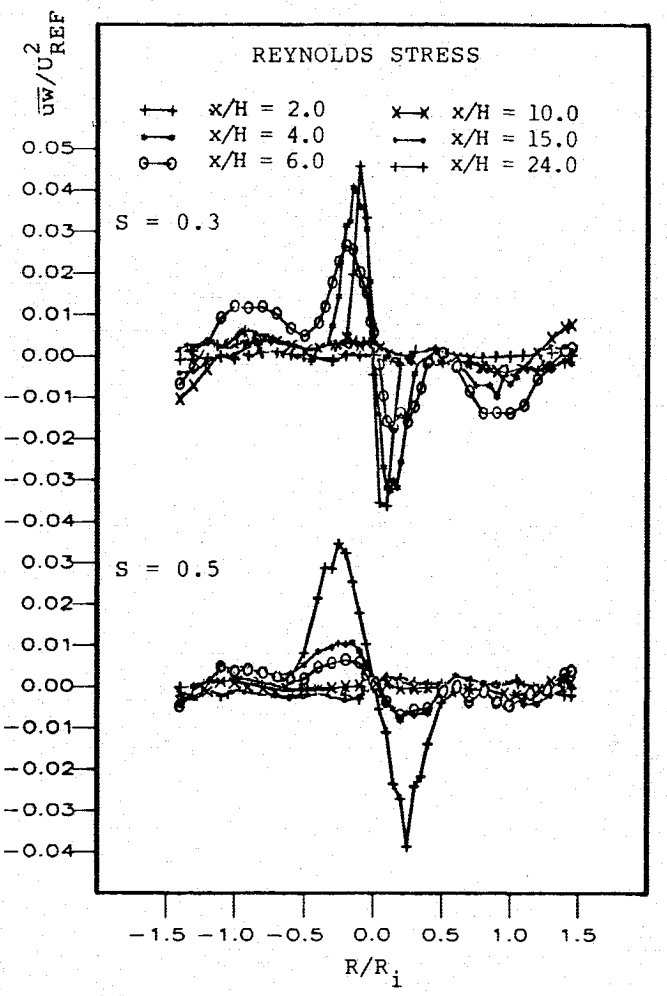

Fig. 8 Reynolds stress profiles.

heights. This could explain the difference in mean tangential flow behavior discussed earlier (see Fig. 5).

Power Spectral Results

Initial power spectral data indicated the existence of distinct peaks at frequencies below 50 Hz for both $S = 0.3$ and $S = 0.5$. Therefore, attention was focused on this frequency range. With a sample rate of 128 Hz, 800 samples were collected at each measurement location, which gave a frequency resolution of better than 0.2 Hz. Power spectrum was averaged over 50 blocks of samples, improving the normalized standard error in power spectrum to better than 15%.

Figure 11 shows power spectral density for both the velocity and acoustic signals for $S = 0.3$. Both cases show a strong peak at approximately 5.25 Hz and its third harmonic at 21 Hz. Only the fundamental structure appears at the vortex core with the third harmonic appearing just outside of the core and becoming stronger toward the combustor wall. This behavior was observed throughout the flowfield up the the last measurement station, which was 24 step heights downstream of the dump plane, but the energy level of these large-scale oscillations decayed in the streamwise direction. Increasing the Reynolds number from 125,000 to about 150,000 increased the fundamental and third harmonic frequencies to approximately 7 and 28 Hz.

To some extent, 0.5 swirl flow showed similar behavior with the fundamental frequency at approximately 9.5 Hz and harmonics at 28.5 and 47.5. The energy contained in these frequencies was an order of magnitude lower than those of $S = 0.3$. Cross-spectral analysis of velocity and acoustic signals showed a coherence function of approximately 0.9 at both the fundamental and harmonic oscillations. In a coaxial confined coswirl and counterswirl flows, Vu and Gouldin[6] reported oscillations on the order of 300 Hz, which they attributed to the rotational frequency of the inner jet. Taking the velocity of the final forced vortex of $S = 0.3$ and the radius of the combustor as characteristic velocity and length gives a rotational frequency of approximately 10 Hz, which is twice the observed oscillation frequency. For 0.5 swirling flow, the vortex core velocity and radius seem to be appropriate characteristic velocity and length. The rotational frequency based on these characteristics is approximately 60 Hz, which is 6 times the observed oscillation frequency. It seems that further research is required to clarify whether or not there is a connection between the observed frequencies and the rotational frequencies.

Garg and Leibovich[32] have investigated in detail the spectral characteristics of vortex breakdown flowfields and reported oscillations in the wake of breakdown with frequencies in the order of those observed in the present experiments. Based on a theoretical analysis by Lessen et al.,[33] Garg and Leibovich showed that these oscillations are associated with nonaxisym-

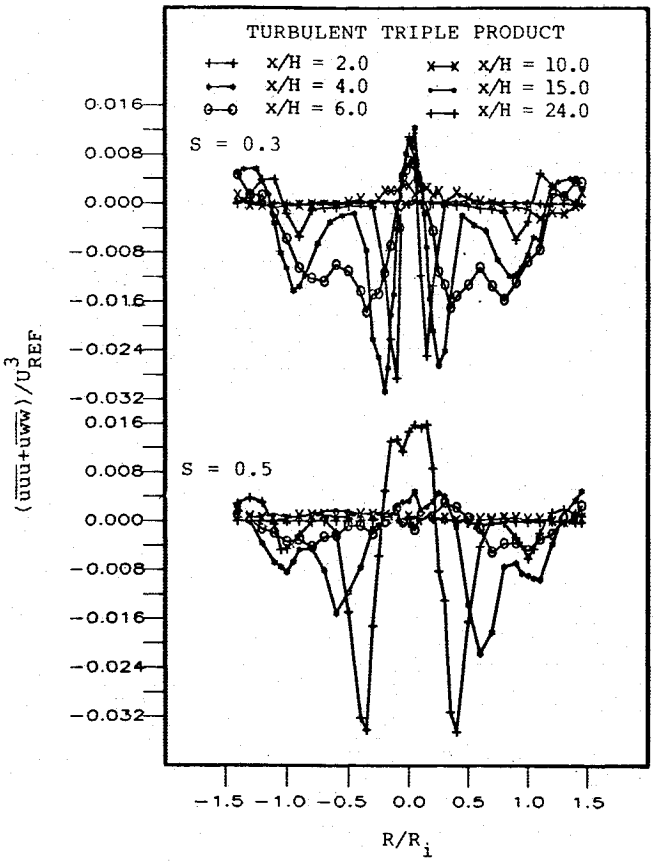

Fig. 9 Axial-convection component of triple correlations of turbulence fluctuations.

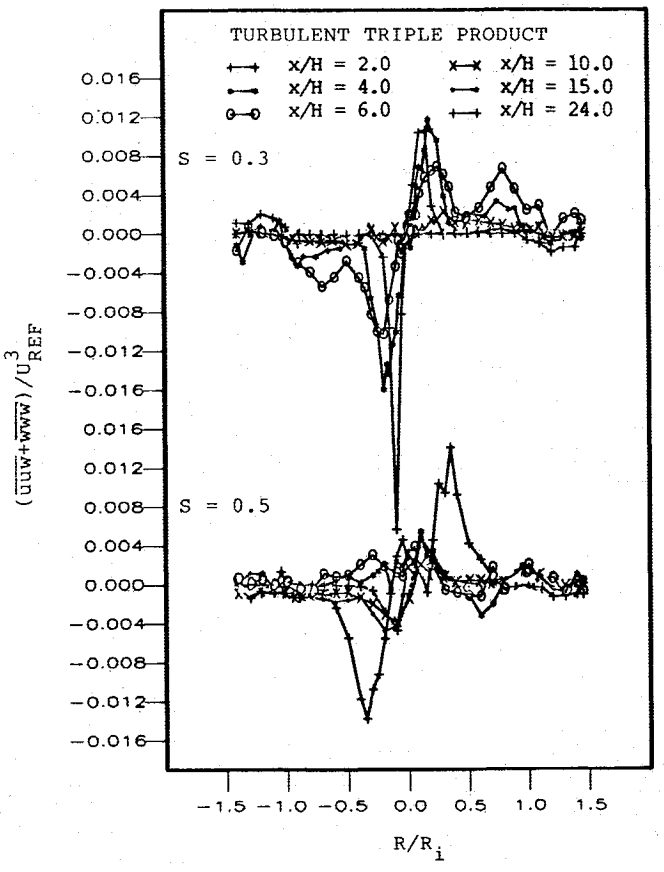

Fig. 10 Tangential-convection component of triple correlations of turbulence fluctuations.

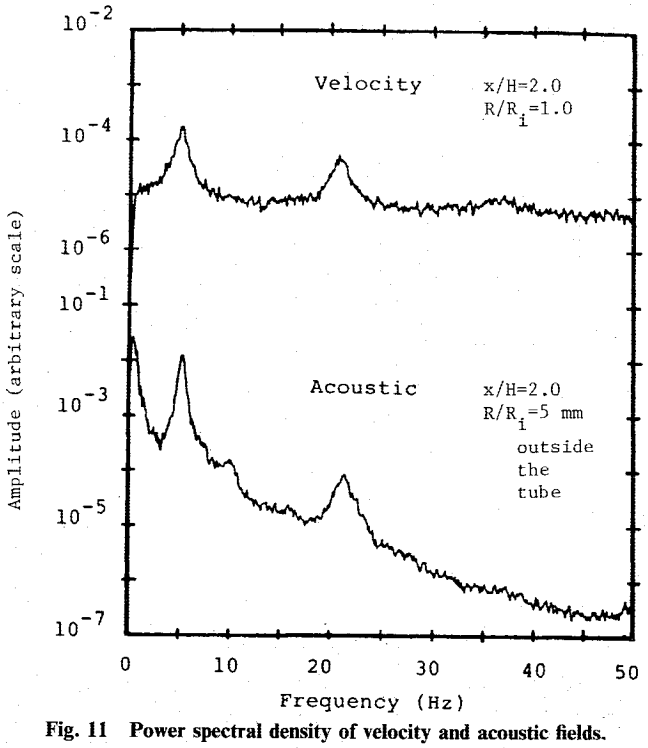

Fig. 11 Power spectral density of velocity and acoustic fields.

metric instabilities in the flowfield. Some preliminary results based on analysis of Lessen et al. show that $S = 0.3$ is stable and $S = 0.5$ is marginally stable for nonaxisymmetric disturbances. This type of analysis might not be applicable to the present flowfields with significant axial velocity developments.

The Ranque-Hilsch or vortex tube,[34] which creates separation in total temperature, has been investigated recently by Kurosaka.[35] He showed that the total temperature separation is due to acoustic streaming induced by nonaxisymmetric orderly disturbances within the swirling flow. Also, he showed that the acoustic streaming is the cause of the deformation of the Rankine vortex of the Ranque-Hilsch tube into a forced vortex. Results of the present experiment, which show an excellent correspondence between the acoustic and velocity spectral characteristics and also deformation of the weaker swirl profile into a forced vortex (see Fig. 5), seem to indicate a direct connection between the acoustic and velocity fields in these swirl flows. Further research is underway to provide some answer to these questions.

IV. Conclusions

A novel experimental setup was used to obtain and document detailed experimental data in a dump combustor configuration with and without swirling inlet flow. A two-component coincident LDV was used and at least 27,300 samples collected to resolve the Reynolds stress and third-order mean products of velocity fluctuations with good accuracy. Reynolds stress results for both $S = 0.3$ and $S = 0.5$ showed values over 20 times higher than those of no swirling flows.

The 0.3 and 0.5 swirling flows with and without centerline flow reversal showed significantly different behaviors. Whereas the 0.5 swirling flow preserved its vortex core strength, the 0.3 swirling flow expanded its vortex core at the expense of losing its strength. Also, the observed coherent large-scale oscillations were much stronger for the weaker swirling flow.

Acknowledgment

This research was supported by the The Air Force Office of Scientific Research under a Universal Energy System Contract F49620-85-C-0013 and a NASA Lewis Contract NAG 3-764.

References

[1]Buckley, P. L., Craig, R. R., Davis, D. L., and Schwartzkopf, K. G., "The Design and Combustion Performance of Practical Swirlers

for Integral Rocket/Ramjets," *AIAA Journal*, Vol. 21, May 1983, pp. 733–740.

[2]Lilley, D. G., "Swirling Flows in Typical Combustor Geometries," AIAA Paper 85-0184, Jan. 1985.

[3]Gouldin, F. C., Depsky, J. S., and Lee, S.-L., "Velocity Field Characteristics of a Swirling Flow Combustor," *AIAA Journal*, Vol. 23, Jan. 1985, pp. 95–102.

[4]Fujii, S., Eguchi, K., and Gomi, M., "Swirling Jets With and Without Combustion," *AIAA Journal*, Vol. 19, Nov. 1981, pp. 1438–1442.

[5]Sislian, J. P. and Cusworth, R. A., "Measurements of Mean Velocity and Turbulent Intensities in Free Isothermal Swirling Jet," *AIAA Journal*, Vol. 24, Feb. 1986, pp. 303–309.

[6]Vu, B. T. and Gouldin, F. C., "Flow Measurements in a Model Swirl Combustor," *AIAA Journal*, Vol. 20, May 1982, pp. 642–651.

[7]Habib, M. A. and Whitelaw, J. H., "Velocity Characteristics of Confined Coaxial Jets With and Without Swirl," *Journal of Fluids Engineering*, Vol. 102, March 1980, pp. 47–53.

[8]Ramos, J. I. and Somer, H. T., "Swirling Flow in a Research Combustor," *AIAA Journal*, Vol. 23, Feb. 1985, pp. 241–248.

[9]Mattingly, J. and Oates, G., "An Experimental Investigation of Co-Annular Swirling Flows," AIAA Paper 85-0186, Jan. 1985.

[10]Kuwatta, M. and Essenhigh, R. H., "Correlation of Pollutant Emissions, Noise, and Heat Transfer in a Natural Gas Combustor," AIAA Paper 75-1267, Oct. 1975.

[11]Rhode, D. L., Lilley, D. G., and McLaughlin, D. K., "Mean Flowfields in Axisymmetric Combustor Geometries with Swirl," *AIAA Journal*, Vol. 21, April 1983, pp. 593–600.

[12]Janjua, S. I. and McLaughlin, D. K., "Turbulence Measurements in a Swirling Confined Jet Flowfield Using a Triple Hot-Wire Probe," Dynamics Technology, Inc., Torrance, CA, Rept. DT-8178-02, 1982.

[13]Beer, J. M. and Chigier, N. A., *Combustion Aerodynamics*, Wiley, New York, 1972.

[14]Gupta, A. K., Lilley, D. G., and Syred, N., *Swirl Flows*, Abacus Press, Turnbridge Wells, England, 1984.

[15]Kilik, E., "Better Swirl Generation by Using Curved Vane Swirlers," AIAA Paper 85-1087, Jan. 1985.

[16]Durrett, R. P., Stevenson, W. H., and Thompson, H. D., "Radial and Axial Turbulent Flow Measurements with an LDV in an Axisymmetric Sudden Expansion Air Flow," *International Symposium on Laser Anemometry*, American Society of Mechanical Engineers, New York, FED Vol. 33, 1985, pp. 127–133.

[17]Craig, R. R., Nejad, A. S., Hahn, E. Y., and Schwartzkopf, K. G., "A General Approach for Obtaining Unbiased LDV Data in Highly Turbulent Non-Reacting and Reacting Flows," AIAA Paper 84-0366, Jan. 1984.

[18]McLaughlin, D. K. and Tiederman, W. G., Jr., "Biasing Correction for Individual Realization of Laser Anemometer Measurements in Turbulent Flows," *The Physics of Fluids*, Vol. 16, No. 12, 1973, pp. 2082–2088.

[19]Petrie, H. L., Samimy, M., and Addy, A. L., "Laser Doppler Velocity Bias in Separated Turbulent Flows," *Journal of Experiments in Fluids*, Vol. 9, No. 2, 1988, pp. 80–88.

[20]Buchhave, P., "The Measurements of Turbulence with Burst Type Laser Doppler Anemometer-Error and Correction Methods," State Univ. of New York at Buffalo, NY, Rept. TRL-196, 1979.

[21]Nejad, A. S. and Davis, D. L., "Velocity Bias in Two-Component Individual Realization Laser Doppler Velocimetry," *Proceedings of the Fifth International Congress on Application of Lasers and Electro Optics*, Arlington, VA, Nov. 1986.

[22]Edwards, R. V. and Jensen, A. S., "Particle-Sampling Statistics in Laser Anemometers: Sample-and-Hold Systems and Saturable Systems," *Journal of Fluid Mechanics*, Vol. 133, 1983, pp. 397–411.

[23]Samimy, M., Petrie, H. L., and Addy, A. L., "A Study of Compressible Turbulent Reattaching Free Shear Layers," *AIAA Journal*, Vol. 24, Feb. 1986, pp. 261–267.

[24]Samimy, M. and Addy, A. L., "Interaction Between Two Compressible Turbulent Free Shear Layers," *AIAA Journal*, Vol. 24, Dec. 1986, pp. 1918–1923.

[25]Smyth, R., "Turbulent Flow Over a Plane Symmetric Sudden Expansion," *Journal of Fluids Engineering*, Vol. 101, Sept. 1979, pp. 348–353.

[26]Eaton, J. K. and Johnston, J. P., "A Review of Research on Subsonic Turbulent Flow Reattachment," *AIAA Journal*, Vol. 19, Sept. 1981, pp. 1093–1100.

[27]Hall, M. G., "The Structure of Vortex Breakdown," *Annual Review of Fluid Mechanics*, Vol. 10, 1972, pp. 195–218.

[28]Leibovich, S., "The Structure of Vortex Breakdown," *Annual Review of Fluid Mechanics*, Vol. 10, No. 46, 1978, pp. 221–246.

[29]Leibovich, S., "Vortex Stability and Breakdown: Survey and Extension," *AIAA Journal*, Vol. 22, Sept. 1984, pp. 1192–1206.

[30]Driver, D. M. and Seegmiller, H. L., "Features of Reattaching Turbulent Shear Layer Subject to Adverse Pressure Gradient," AIAA Paper 82-1029, 1982.

[31]Chandrsuda, C. and Bradshaw, P., "Turbulence Structure of a Reattaching Mixing Layer," *Journal of Fluids Mechanics*, Vol. 110, 1981, pp. 171–194.

[32]Garg, A. K. and Leibovich, S., "Spectral Characteristics of Vortex Breakdown Flowfields," *Physics of Fluids*, Vol. 22, No. 11, 1979, pp. 2053–2064.

[33]Lessen, M., Singh, P. J., and Paillet, F., "The Stability of a Trailing Line Vortex. Part 1. Inviscid Theory," *Journal of Fluid Mechanics*, Vol. 63, Pt. 4, 1974, pp. 753–763.

[34]Hilsch, R., "The Use of Expansion of Gases in a Centrifugal Field as Cooling Process," *Review of Scientific Instruments*, Vol. 18, No. 2, 1947, pp. 108–113.

[35]Kurosaka, M., "Acoustic Streaming in Swirling Flow and the Ranque-Hilsch (Vortex-Tube) Effect," *Journal of Fluids Mechanics*, Vol. 124, 1982, pp. 139–172.